

Wave packet dynamics of nonlinear Gazeau-Klauder coherent states of a position-dependent mass system in a Coulomb-like potential

Faustin Blaise Migueu, Mercel Vubangsi, Martin Tchoffo, and Lukong Cornelius Fai

Citation: Chin. Phys. B, 2021, 30 (**6**): 060309. DOI: 10.1088/1674-1056/abd7e2
Journal homepage: http://cpb.iphy.ac.cn; http://iopscience.iop.org/cpb

What follows is a list of articles you may be interested in

Exact solution of the (1+2)-dimensional generalized Kemmer oscillator in the cosmic string background with the magnetic field

Yi Yang(杨毅), Shao-Hong Cai(蔡绍洪), Zheng-Wen Long(隆正文), Hao Chen(陈浩), Chao-Yun Long(龙超云)
Chin. Phys. B, 2020, 29 (**7**): 070302. DOI: 10.1088/1674-1056/ab888e

Generating Kerr nonlinearity with an engineered non-Markovian environment

Fei-Lei Xiong(熊飞雷), Wan-Li Yang(杨万里), Mang Feng(冯芒)
Chin. Phys. B, 2020, 29 (**4**): 040302. DOI: 10.1088/1674-1056/ab7741

Solution of the spin-one DKP oscillator under an external magnetic field in noncommutative space with minimal length

Bing-Qian Wang(王炳乾), Zheng-Wen Long(隆正文), Chao-Yun Long(龙超云), Shu-Rui Wu(吴淑蕊)
Chin. Phys. B, 2018, 27 (**1**): 010301. DOI: 10.1088/1674-1056/27/1/010301

Superconducting phase qubits with shadow-evaporated Josephson junctions

Fei-Fan Su(宿非凡), Wei-Yang Liu(刘伟洋), Hui-Kai Xu(徐晖凯), Hui Deng(邓辉), Zhi-Yuan Li(李志远), Ye Tian(田野), Xiao-Bo Zhu(朱晓波), Dong-Ning Zheng(郑东宁), Li Lv(吕力), Shi-Ping Zhao(赵士平)
Chin. Phys. B, 2017, 26 (**6**): 060308. DOI: 10.1088/1674-1056/26/6/060308

Design of a gap tunable flux qubit with FastHenry

Naheed Akhtar, Yarui Zheng(郑亚锐), Mudassar Nazir, Yulin Wu(吴玉林), Hui Deng(邓辉), Dongning Zheng(郑东宁), Xiaobo Zhu(朱晓波)
Chin. Phys. B, 2016, 25 (**12**): 120305. DOI: 10.1088/1674-1056/25/12/120305

Wave packet dynamics of nonlinear Gazeau–Klauder coherent states of a position-dependent mass system in a Coulomb-like potential

Faustin Blaise Migueu[1], Mercel Vubangsi[1,2], Martin Tchoffo[1,3,†], and Lukong Cornelius Fai[1]

[1] *Unité de Recherche de Matière Condensée, d'Électronique et de Traitement du Signal, Département de Physique, Faculté des Sciences, Université de Dschang, B.P: 67, Dschang, Cameroon*

[2] *Computational Material Science Laboratory, Higher Technical Teachers' Training College Bambili, University of Bamenda, PO Box 39, Bamenda, Cameroon*

[3] *Centre d'Études et de Recherches en Agronomie et en Biodiversité, Université de Dschang, Dschang, Cameroon*

(Received 13 October 2020; revised manuscript received 2 December 2020; accepted manuscript online 4 January 2021)

A $D = 1$ position-dependent mass approach to constructing nonlinear quantum states for a modified Coulomb potential is used to generate Gazeau–Klauder coherent states. It appears that their energy eigenvalues are scaled down by the quantum number and the nonlinearity coefficient. We study the basic properties of these states, which are found to be undefined on the whole complex plane, and some details of their revival structure are discussed.

Keywords: deformed Coulomb potential, energy spectrum, coherent states, photon number distribution, quantum revivals

PACS: 03.65.Ge, 21.10.Sf, 42.50.Md **DOI:** 10.1088/1674-1056/abd7e2

1. Introduction

We have known for a long time that in semiconductor lattices, charge carriers such as electrons or holes behave as if their masses have been altered, compared to their vacuum masses. The so-called effective mass possesses anisotropy, and it sometimes appears to be negative.[1–7] The study of effective masses has gained importance in recent times, because the control of semiconductor materials is the origin of modern information and communications. Due to the recent development of devices that exhibit interesting quantum effects, physical systems with variable masses have emerged. In particular, systems with position-dependent masses play a major part in quantum wells, heterostructures, inhomogeneous doped semiconductors, quantum liquids, graded crystals, nanoscale quantum rings, etc.[8] Nevertheless, the quantization of such systems encounters serious mathematical challenges, due to complexity encountered during the resolution of eigenfunction equations. More precisely, the task of prospective generalization of the standard hamiltonian using variable mass theory is made difficult by the fact that the momentum and mass operators do not commute. A number of physical variable-mass scenarios exist. An illustrative case has been pointed out by Wang *et al.*, who provided evidence that the Schrödinger equation for a thin charged envelope moving in an appropriate gravitational field can be likened to a coordinate-dependent mass problem.[9] The literature overflows with techniques for investigating such problems. Among them, one can cite point canonical transformation, factorization by the supersymmetry method, the displacement operator approach, Lie algebraic parametrization, the Nikiforov–Uvarov method, the path integral approach, etc.[10–14] The commutation relation between the position operator and the momentum induces ordering ambiguities in the kinetic energy operator, giving rise to various forms of hamiltonian, as shown in Refs. [15–19]. The history of quantum mechanics is long and deep, but the comprehension of singular potentials remains less extensive. This is the case for $D = 1$ Coulomb problems x^{-1}, for which, all solutions should satisfy the wave equation over the whole of the x-axis, including the origin. The results of this class of problem are significant, theoretically as well as experimentally, although the literature abounds with related controversial statements.[20–26] Quantum mechanical systems with variable masses are not yet mastered, although voluminous research has been conducted on the subject. A hot topic for experts is the limit between classical mechanics and quantum physics. In the early days of quantum theory, this question was investigated by Erwin Schrödinger, who established a correspondence between classical and quantum dynamics with a minimum uncertainty using the framework of the harmonic oscillator. However, he did not extend this minimum uncertainty to all physical systems. After a period of hibernation of more than three decades, Roy Glauber had the ingenious idea of expressing these minimum uncertainty states in terms of the raising and lowering operators of the harmonic oscillator.[2,3,27,28] These states were given the name coherent states and then generalized to systems much more complicated than the harmonic oscillator in various fields of physics, such as quantum electrodynamics, quantum optics, quantum processing, quantum information and computation, etc. In most textbooks today, one comes across the following definitions of coherent

†Corresponding author. E-mail: mtchoffo2000@yahoo.fr

© 2021 Chinese Physical Society and IOP Publishing Ltd

states: (i) eigenstates of the lowering operator; (ii) states resulting from the displacement operator's action on the vacuum; (iii) states that minimize the Heisenberg–Robertson uncertainty relation and (iv) states that satisfy Gazeau–Klauder natural conditions by constituting an overcomplete family of vectors in the Hilbert space of the harmonic oscillator.[29–32] Coherent states of this fourth class are recognized to fulfill the temporal stability and action identity conditions. In Ref. [29], it is emphasized that Gazeau–Klauder coherent states have emerged as the most important for the analysis of physical systems and should survive if one puts aside coherent state properties. In this work, we focus on Gazeau–Klauder coherent states which have previously been studied for constant-mass systems, but have not yet captivated the attention of researchers for use in variable mass systems, apart from a few scientific publications.

This paper is structured as follows. In Section 2, we start by presenting the model of the studied system, the energy eigenvalues and also the bound state eigenfunctions of the underlying system; Section 3 is devoted to the generation of Gazeau–Klauder coherent states and an investigation of their basic properties by means of the probability distribution of photons in the configuration space; the main purpose of Section 4 is an inquiry into some aspects of the previously constructed coherent states during their time evolution. We end this communication by summarizing our results in Section 5.

2. System model and generation of the energy eigenvalues

2.1. Derivation of the energy spectrum

In the context of semiconductor heterostructures, unidimensional position dependent mass Schrödinger equations were proposed in the 1980s, based on von Roos' idea and set up in terms of ambiguity numbers a_1, a_2 and a_3 constrained as $a_1+a_2+a_3=-1$, that is,[33]

$$\left[\frac{1}{4}\left(m^{a_1}(x)\hat{p}m^{a_2}(x)\hat{p}m^{a_3}(x)+m^{a_3}(x)\hat{p}m^{a_2}(x)\hat{p}m^{a_1}(x)\right)+V(x)\right]\phi_n(x)=E_n\phi_n(x), \tag{1}$$

where the momentum operator $\hat{p}=-\mathrm{i}\hbar\,\mathrm{d}/\mathrm{d}x$, E_n is the energy spectrum of the system under consideration and $\phi_n(x)$ denotes its eigenfunctions, which provide us with the probability amplitude for the charge carrier to be at a position x along the axis. $V(x)$ stands for the potential that describes the space in which the studied quantum particle evolves. One can write another closed form of $\hat{p}$, the momentum operator, so that the equation becomes[34]

$$-\frac{\hbar^2}{2}\frac{1}{\sqrt{m(x)}}\frac{\mathrm{d}}{\mathrm{d}x}\frac{1}{\sqrt{m(x)}}\frac{\mathrm{d}}{\mathrm{d}x}\phi_n(x)+V(x)\phi_n(x)=E_n\phi_n(x). \tag{2}$$

It is possible to connect Eq. (2) with the von Roos kinetic energy operator presented in the coordinate dependent mass Schrödinger Eq. (1) through a hermitization scheme introduced by Mustafa-Mazharimousavi,[35] leading to the ordering ambiguity parameter set of $a_1=a_2/2=a_3=-1/4$. Our particle, investigated hereafter, is designated as a space variable-effective-mass charge carrier with an effective mass expressed by the following numerical law:

$$m(x)=m_0\left(\frac{\lambda^2x^2}{1+\lambda^2x^2}\right), \tag{3}$$

in which m_0 is the carrier vacuum mass and λ represents the space deformation coefficient with the inverse length dimension. This gauges the accuracy of the link between the carrier's effective mass and the coordinate. We assume this charge carrier to be moving in a quantum space modeled by a Coulomb–type potential given by

$$V(x)=-\frac{V_0}{\sqrt{1+\beta x^2}}, \tag{4}$$

in which the singularity has been lifted off, compared to the standard Coulomb one. The β-parameter with a squared inverse length dimension evaluates the impact of the coordinate on the potential. Such an alteration in the potential renders the problem more realistic, as well as bypassing the troublesome Dirichlet conditions.[36] The idea here is to model the system with a renormalized form of the Coulomb potential which is physically easier to implement. Fig. 1 is a plot of the mass profile as well as the variations of the quantum potential defined by Eq. (4). From curve (i), it can be seen that the carrier's effective mass is zero at the coordinate origin, but equal to the vacuum mass when the particle is distant from that position. Such a situation is recurrent in heterostructures. In the case of curve (ii), the particle experiences a potential with fewer impurities than in case (iii). With fewer impurities, the carrier moves more freely along the chain. It is worth pointing out that the more impurities, the deeper the potential well. Such a potential has been studied in Ref. [37] using soliton features in doped trans-polyacetylene $(CH)_v$, assumed to be a matrix of parallel linear chains with no inter-chain conduction. To generate the bound states of the system in the $\beta=\lambda^2$ scenario,

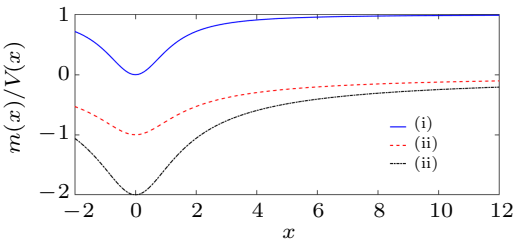


Fig. 1. Plot of the mass function (i) and the confinement potentials $V_0=1$ (ii), $V_0=2$ (iii) versus the position of the charge carrier for $\beta=0.64$, $\lambda=0.80$ and $m_0=1$.

let us substitute Eqs. (3) and (4) into Eq. (2) and then perform the following independent variable changes:

$$z = \frac{2}{\lambda\hbar}\sqrt{-2m_0E_n}\sqrt{1+\lambda^2x^2};$$
$$\alpha = -\frac{V_0}{\lambda\hbar}\sqrt{-\frac{m_0}{2E_n}}. \tag{5}$$

It follows after careful calculation that the Schrödinger wave equation (2) is equivalent to

$$\frac{\mathrm{d}^2\phi_n(z)}{\mathrm{d}z^2} + \left(\frac{\alpha}{z} - \frac{1}{4}\right)\phi_n(z) = 0. \tag{6}$$

By taking into account the asymptotic behavior of the energy eigenvector solutions of Eq. (6) for $z \gg 1$, we choose the ansatz

$$\phi_n(z) = f(z)\mathrm{e}^{-z/2}, \tag{7}$$

resulting in Kummer's equation

$$\left(z\frac{\mathrm{d}^2}{\mathrm{d}z^2} - z\frac{\mathrm{d}}{\mathrm{d}z} + \frac{\alpha}{2}\right)f(z) = 0. \tag{8}$$

Equation (8) is solvable only if the parameter α is constrained to be an integer [38,39]. Since $f(z)$ is expected to be a single hypergeometric function ${}_1\mathrm{F}_1$, therefore $\alpha = n+1$, $n = 0, 1, 2$, etc. Consequently, Eq. (5) yields

$$E_n = -\frac{m_0V_0^2}{2\lambda^2\hbar^2(n+1)^2}. \tag{9}$$

The result of Eq. (9) is satisfactory insofar as it is consistent with the $1/n^2$ dependence of the energy spectrum previously seen in many other Coulomb problems.[20,22,26,40–44] Furthermore, one notes that these energy eigenvalues are proportional to the strength V_0 of the confinement potential but, are scaled down by the space deformation coefficient λ. Let us use the analytic procedure to solve Eq. (8).

2.2. Traditional method to complete solutions

We assume the solution $f(z)$ as the Frobenius series

$$f(z) = \sum_{r=0}^{+\infty} w_r z^{r+r_0}. \tag{10}$$

The motivation for choosing the Frobenius approach is that the number r_0 can be zero or any rational number. The first and second derivatives of Eq. (10) with respect to z, carefully introduced into Eq. (8), provide us with the following recursive relation:

$$(r+r_0-1)(r+r_0)w_r = [(r+r_0-1) - \alpha/2]\,w_{r-1}. \tag{11}$$

It can be seen that the lowest power of z is derived from $r = 0$. Thus, $r_0(r_0-1) = 0$. The case $r_0 = 0$ has been put aside, since it leads to meaningless terms. Thus,

$$w_r = \frac{r-\alpha/2}{r(r+1)}w_{r-1}, \tag{12}$$

appears as a suitable solution. Trying few iterations,

$$w_1 = \frac{(1-\alpha/2)}{1\times 2}w_0;\ \ w_2 = \frac{(1-\alpha/2)(2-\alpha/2)}{1\times 2^2\times 3}w_0;\ \ \cdots \tag{13}$$

leads to the following general coefficient:

$$w_n = \frac{(1-\alpha/2)_n}{n!(n+1)!}w_0, \tag{14}$$

that permits Eq. (10) to yield $f(z)$ as

$$f(z) = \sum_{n=0}^{+\infty} w_0 \frac{(1-\alpha/2)_n}{(2)_n}\frac{z^{n+1}}{n!}, \tag{15}$$

which exactly matches our expectation of $f(z)$ being a ${}_1\mathrm{F}_1$ confluent hypergeometric function. Equation (15) can then be introduced into Eq. (7) to finally give the general solutions of the wave equation as

$$\phi_n(z) = zw_0\mathrm{e}^{-z/2}{}_1\mathrm{F}_1(1-\alpha/2;2;z). \tag{16}$$

The eigenfunctions of coordinate space $\phi_n(z)$ admit the following boundary conditions:

$$\phi_n(0) = 0;\ \ \phi_n(+\infty) = 0;\ \ \phi_n'(0) = \frac{1}{\sqrt{K(\alpha)}}, \tag{17}$$

with the constraint $z \geq 0$, the prime ($'$) denotes a derivative with respect to z and $w_0 = 1/\sqrt{K(\alpha)}$. So far,

$$\phi_n(z) = \frac{z\mathrm{e}^{-z/2}}{\sqrt{K(\alpha)}}{}_1\mathrm{F}_1(1-\alpha/2;2;z). \tag{18}$$

The normalization constant has been calculated using the standard condition as $\int_0^\infty \phi_n^*(z)\phi_n(z)\,\mathrm{d}z = 1$, that is consistent with the constraint on the z-variable. It follows that[45]

$$K(\alpha) = \sum_{k=0}^{+\infty}\sum_{j=0}^{k}\frac{(1-\alpha/2)_j(1-\alpha/2)_{k-j}}{(2)_j(2)_{k-j}}\frac{(k+2)!}{j!(k-j)!}. \tag{19}$$

An alternative approach would be to consider a deformed space

$$x_\lambda = \int^x \sqrt{\frac{m(\omega)}{m_0}}\,\mathrm{d}\omega = \frac{\sqrt{1+\lambda^2x^2}}{\lambda}. \tag{20}$$

Thus, the transformation $x \to x_\lambda$ changes the problem of a charge carrier with variable mass trapped in a deformed potential (4), into that of a charge carrier with a constant-mass confined in a standard Coulombian potential, say

$$-\frac{\hbar^2}{2m_0}\frac{\mathrm{d}^2\psi_n(x_\lambda)}{\mathrm{d}x_\lambda^2} - \frac{V_0}{\lambda}\frac{1}{x_\lambda}\psi_n(x_\lambda) = E_n\psi_n(x_\lambda), \tag{21}$$

with $\psi_n(x_\lambda) = \phi_n(x(x_\lambda))$. The solutions of the one-dimensional problem stated in Eq. (21) have been discussed

in Refs. [46,47] in terms of the associated Laguerre polynomials $L_n^{(\nu)}$

$$\phi_n(x_\lambda) = K(n)\frac{x_\lambda}{nx_0}\mathrm{e}^{-x_\lambda/2}L_{n-1}^{(1)}\left(\frac{x_\lambda}{nx_0}\right),$$
$$K(n) = \frac{1}{\sqrt{2n^3x_0}},\ x_0 = \frac{\lambda\hbar^2}{2mV_0}. \tag{22}$$

The solutions to problems (4) and (21) are isospectral. This view gives a physical meaning to the deformed 1D Coulomb-like problem studied. In addition, the solution given by Eq. (22) permits a compact form of the normalization constant $K(n)$ to be obtained by means of the orthogonality condition of the associated Laguerre polynomials.

We now have sufficient materials to build coherent Gazeau–Klauder states in Section 3 of this communication.

3. Coherent Gazeau–Klauder states of the system and their properties

3.1. Generation of Gazeau–Klauder coherent states

Unlike other coherent states such as Barut–Girardello's or Perelomov's which are constructed on the basis of Lie groups, Gazeau–Kauder coherent states are not associated with any algebraic group. For any Hermitian Hamiltonian of eigenstates $|\phi_n\rangle$, the unique cornerstone of Gazeau–Klauder coherent-state $|s,\xi\rangle$ building is the energy spectrum of the system in question. Minimal parameterizations enabled Gazeau and Klauder to denote their coherent states by[32]

$$|s,\xi\rangle = \frac{1}{\sqrt{G(s)}}\sum_{n=0}^{+\infty}\frac{s^{n/2}\mathrm{e}^{-\mathrm{i}\xi e_n}}{\sqrt{\theta_n}}|\phi_n\rangle, \tag{23}$$

in which s is the coherent state parameter constrained to belong to the disk $\{s\in\mathcal{C},\ |s|<R\}$. R denotes the radius of convergence of the previous series, ξ is the angular variable and $\theta_n = e_1\times e_2\times\ldots\times e_n$ with e_n known as the dimensionless energy of the system, expressed as

$$e_n = \frac{1}{\varepsilon}(E_n - E_0). \tag{24}$$

The parameter ε with the energy dimension is introduced to scale e_n, rendering it dimensionless. Consequently, Eq. (24) together with Eq. (9) provide us with

$$e_n = \frac{m_0V_0^2}{2\varepsilon\lambda^2\hbar^2}\left(1-\frac{1}{(n+1)^2}\right), \tag{25}$$

leading to the computation of the product θ_n of the dimensionless energies as

$$\theta_n = \prod_{k=1}^{n}e_k = \frac{a^n}{2}\frac{n+2}{n+1},\ \theta_0 = 1. \tag{26}$$

It is obvious that for the sake of simplicity, we have set a as the modified space deformation coefficient, say

$$a = \frac{m_0V_0^2}{2\varepsilon\lambda^2\hbar^2}. \tag{27}$$

On the other hand, the normalization factor $G(s)$ will be obtained on the basis of the standard condition stated as $\langle s,\xi|s,\xi\rangle = 1$. It then follows from Eq. (23) that

$$G(s) = \sum_{n=0}^{+\infty}\frac{s^n}{\theta_n}. \tag{28}$$

Elements from Eqs. (26) and (28) can be connected to generate an elegant form of this normalization factor in terms of a confluent hypergeometric function, say

$$G(s) = {}_2\mathrm{F}_1\left(2,2;3;\frac{s}{a}\right). \tag{29}$$

Substituting Eq. (26) into Eq. (23) yields the family of states we seek to study

$$|s,\xi\rangle = \sqrt{\frac{2}{G(s)}}\sum_{n=0}^{+\infty}\sqrt{\frac{n+1}{n+2}}\mathrm{e}^{-\mathrm{i}\xi e_n}\left(\frac{s}{a}\right)^{n/2}|\phi_n\rangle. \tag{30}$$

Stated otherwise, the expression given in Eq. (30) stands for the Gazeau–Klauder coherent states of our position-dependent mass system confined in the Coulomb-like potential given in Eq. (4).

3.2. Basic properties of Gazeau–Klauder coherent states

A suitable way to probe the existence of such a series solution is to compute the radius of convergence R, as follows:[32]

$$R = \lim_{n\to+\infty}\sqrt[n]{\theta_n}. \tag{31}$$

Using Eq. (26) in Eq. (31), a straightforward calculation shows that $R = a$, which is an interesting feature. Thus, we can argue that Gazeau–Klauder coherent states for the position dependent-mass system under consideration do exist, but are not defined on the whole complex plane. This result is not surprising if one takes a closer look at the energy shape in Eq. (25). In agreement with Eq. (30) the scalar product between two representatives $|s,\xi\rangle$ and $|s',\xi'\rangle$ of the Gazeau–Klauder coherent-state family reads

$$\langle s,\xi|s',\xi'\rangle = \frac{2}{\sqrt{G(s')}\sqrt{G(s)}}\sum_{n=0}^{+\infty}\frac{n+1}{n+2}\times\mathrm{e}^{-\mathrm{i}(\xi'-\xi)e_n}\left(\frac{s's}{a^2}\right)^{n/2}. \tag{32}$$

The latter real-valued expression $s's$ cannot vanish. So, the previous overlap is a non-zero number. Consequently, the Gazeau–Klauder coherent states for the studied position-dependent mass system do not form an orthogonal family. The family $\{|s,\xi\rangle\}$ is therefore said to be overcomplete. Apart from overcompleteness, the continuity property is another Klauder minimum requirement for a family of states to be

termed coherent.[48] Here, continuity has a peculiar connotation, say, for a family mapping, such that $|s,\xi\rangle \to |s',\xi'\rangle$, it follows that $||\,|s,\xi\rangle - |s',\xi'\rangle\,|| \to 0$. Adapting the previous definition to our problem of a Coulomb-like potential induces the following norm:

$$||\,|s,\xi\rangle - |s',\xi'\rangle\,|| = \sqrt{2\left[1 - \mathrm{Re}\,\langle s,\xi|s',\xi'\rangle\right]} \tag{33}$$

which tends to zero for $|s,\xi\rangle$ approaching $|s',\xi'\rangle$. As a strong point of this result, we assert that the family of vectors $\{|s,\xi\rangle\}$ forms a continuous and connected submanifold in the configuration space.

3.3. Statistical properties of Gazeau–Klauder coherent states

The statistical features of the Gazeau–Klauder coherent states for the studied position-dependent mass system can be investigated through the photon number distribution σ_n, defined as the squared modulus of the weighting coefficient of Eq. (30), that is,

$$\sigma_n = \frac{2}{{}_2\mathrm{F}_1\left(2,2;3;\frac{s}{a}\right)}\left(\frac{s}{a}\right)^n \frac{n+1}{n+2}. \tag{34}$$

The mean excitation number is defined as the first moment of the photon number distribution, as

$$\langle n\rangle = \sum_{n=0}^{+\infty} n\sigma_n, \tag{35}$$

that has been computed and then expressed in terms of the confluent hypergeometric functions as

$$\langle n\rangle = \left(\frac{8s}{3a}\right)\frac{{}_2\mathrm{F}_1\left(3,3;4;\frac{s}{a}\right)}{{}_2\mathrm{F}_1\left(2,2;3;\frac{s}{a}\right)}. \tag{36}$$

In a similar manner, the second moment of the photon number distribution reads

$$\langle n^2\rangle = \sum_{n=0}^{+\infty} n^2\sigma_n \tag{37}$$

equivalent to

$$\langle n^2\rangle = \left(\frac{8s}{3a}\right)\frac{{}_3\mathrm{F}_2\left(2,3,3;1,4;\frac{s}{a}\right)}{{}_2\mathrm{F}_1\left(2,2;3;\frac{s}{a}\right)}. \tag{38}$$

It is henceforth an easy task to derive the variance $(\Delta n)^2 = \langle n^2\rangle - \langle n\rangle^2$ of the distribution from Eqs. (36) and (38) as

$$(\Delta n)^2 = \frac{\left(\frac{8s}{3a}\right)}{{}_2\mathrm{F}_1\left(2,2;3;\frac{s}{a}\right)}\left[{}_3\mathrm{F}_2\left(2,3,3;1,4;\frac{s}{a}\right) - \frac{\left(\frac{8s}{3a}\right)}{{}_2\mathrm{F}_1\left(2,2;3;\frac{s}{a}\right)}\left[{}_2\mathrm{F}_1\left(3,3;4;\frac{s}{a}\right)\right]^2\right]. \tag{39}$$

All the requisites contained in Eqs. (34), (36), and (38) stand for the basic elements required to gain insight into the statistical behavior of our system. For this purpose, we have started by plotting in Fig. 2 the photon number distribution σ_n as a function of the quantum number n for various values of the Gazeau–Klauder coherent-state parameter s and the nonlinearity coefficient a. It can be seen that the distribution is a deformed Poissonian. This was to be expected, due to the fact that the system possesses a Coulomb spectrum. In addition, a simple observation of Fig. 2 shows that, for all values of s, the σ_n-curve is narrower than the standard Poissonian. This points out the sub-Poissonian nature of our distribution.[3,8] Figure 3 shows that no matter how the nonlinearity coefficient a changes, the mean of the photon number distribution remains greater than its variance. This observation clearly indicates that the distribution is not Poissonian. Nervertheless, for small values of the coherent state parameter, the mean and the variance of the distribution evolve towards a point of coincidence. It appears in the previous figure that the mean $\langle n\rangle$ of the distribution and Gazeau–Klauder coherent-state parameter s are two quantities that are proportional to each other. The Mandel parameter Q is an interesting instrument for classification of the photon number distribution. In fact, the distribution is

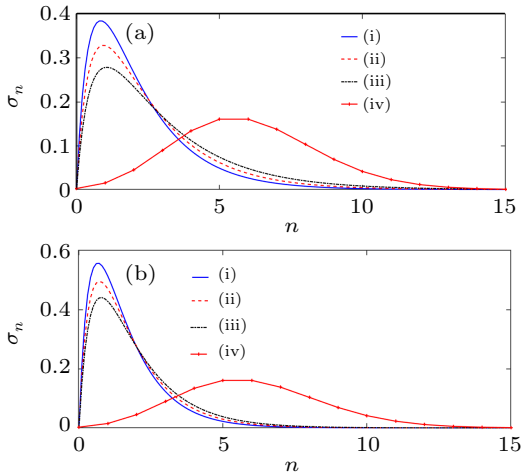


Fig. 2. Plot of the photon number distribution σ_n versus the quantum number n for (i) $s = 0.010$, (ii) $s = 0.011$, (iii) $s = 0.012$ and (iv) the standard Poissonian in the contexts of (a) $a = 0.019$ and (b) $a = 0.025$.

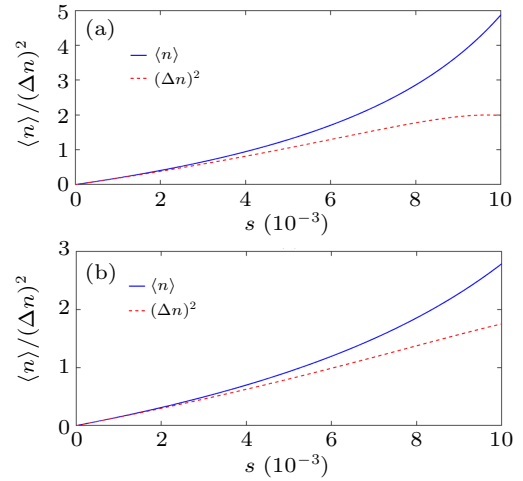


Fig. 3. Plot of the mean and the variance of the photon number distribution versus the coherent-state parameter s for (a) $a = 0.015$ and (b) $a = 0.019$.

Poissonian for $Q=0$, super-Poissonian for $Q>0$ and sub-Poissonian if $Q<0$.[49,50] This parameter is given by

$$Q=\frac{\langle n^2\rangle-\langle n\rangle^2-\langle n\rangle}{\langle n\rangle}, \tag{40}$$

and matches with

$$Q=\frac{1}{{}_2\mathrm{F}_1\left(3,3;4;\frac{s}{a}\right)}\left[{}_3\mathrm{F}_2\left(2,3,3;1,4;\frac{s}{a}\right)-\frac{\left(\frac{8s}{3a}\right)}{{}_2\mathrm{F}_1\left(2,2;3;\frac{s}{a}\right)}\left[{}_2\mathrm{F}_1\left(3,3;4;\frac{s}{a}\right)\right]^2\right]-1, \tag{41}$$

plotted in Fig. 4(a). The latter figure shows that $Q<0$ in the present case. Consequently, the Gazeau–Klauder coherent states for the position-dependent mass are subject to sub-Poissonian statistics. In other words, the expected value of the photon number is always larger than its fluctuations. The previous result can be strengthened by studying the last parameter, called the second-order correlation function, $g^2(0)$ given as

$$g^2(0)=\frac{\langle n^2\rangle-\langle n\rangle^2}{\langle n\rangle}, \tag{42}$$

that, in this case, is identical to:

$$g^2(0)=\frac{{}_3\mathrm{F}_2\left(2,3,3;1,4;\frac{s}{a}\right)}{{}_2\mathrm{F}_1\left(3,3;4;\frac{s}{a}\right)}-\left(\frac{8s}{3a}\right)\frac{{}_2\mathrm{F}_1\left(3,3;4;\frac{s}{a}\right)}{{}_2\mathrm{F}_1\left(2,2;3;\frac{s}{a}\right)}, \tag{43}$$

as plotted in Fig. 4(b). It is well known that a distribution is Poissonian for $g^2(0)=1$, super-Poissonian for $g^2(0)>1$ and sub-Poissonian if $g^2(0)<1$.[49–52] The case we are dealing with, $g^2(0)<1$, evidently confirms the sub-Poissonian nature of the photon number distribution, no matter the change in the nonlinearity coefficient a.

We now conclude this section by noting that the Gazeau–Klauder coherent states for the position-dependent mass system trapped in a Coulomb-like potential exhibit an effect that has no analog in classical mechanics, the anti-bunching phenomenon.[53]

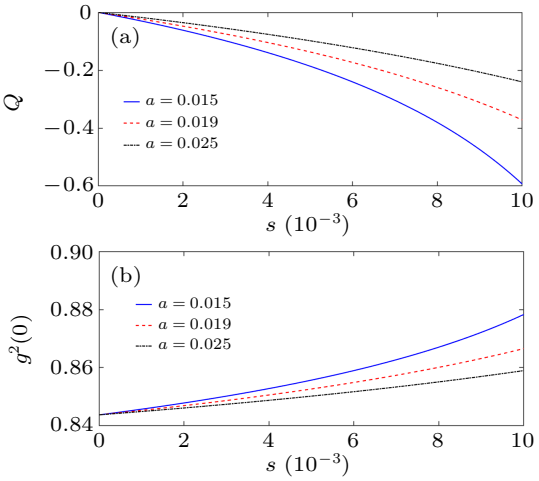


Fig. 4. Plots of (a) the Mandel parameter and (b) the second-order correlation function versus s for various values of the modified nonlinearity coefficient a.

4. Temporal evolution of Gazeau–Klauder coherent states

4.1. Time scales in wave packets evolution

Quantum states are expected to show a recurrent behavior, consisting of a series of collapses alternating with revivals as the time passes.[54–56] The structure of these recurrences is strongly linked to the energy eigenvalues of the relevant system. It is well known that an individual eigenstate is stationary, and consequently exhibits no motion. On the contrary, a wave packet that is localized in a space admits variable expectation values as time evolves. One says that localized wave packets are dynamically nonstationary. It is worthwhile pointing out that the propagation of the previous wave packet is framed by the correspondence principle, which asserts that classical and quantum mechanics must agree in the context of highly excited states. Hereafter, we hold wave packet dynamics to be a strong tool for the study of our system's time evolution. The motion of wave packets of energy values e_n localized around a central quantum number n_0 is governed by the important timescales defined as

$$t^{(k)}=2\pi\hbar\left(\left|\frac{1}{k!}\frac{\mathrm{d}^k e_n}{\mathrm{d}n^k}\right|^{-1}\right)_{n=n_0},\quad k=1,2,3,\ldots, \tag{44}$$

such that $t^{(k)}<t^{(k+1)}$. A proof of this inequality is provided in the Appendix. To obtain $t^{(k)}$, we write the energy in terms of the Taylor series with respect to the quantum number n through a finite order. After this, we find times that cause the wave function's phase to be a multiple of 2π. Here, $t^{(1)}$ is the classical period of the motion denoted by t_c, $t^{(2)}$ stands for the revival timescale denoted by t_r and $t^{(3)}$ is the super revival timescale, recorded as t_s hereafter. In the special case of the harmonic oscillator the wave packet never fully collapses and there are no revivals.[57,58] Systems such as the rigid rotator, the infinite well, etc., that record an energy expression quadratic in the quantum number, undergo collapses and quantum revivals on a timescale t_r. More realistic physical systems, such as Rydberg clusters are recognized to display more complicated revival patterns.[58,59] A study of the role of terms in the Taylor expansion of the energy is provided by Ref. [60], in which it is shown that at the times $t\approx(n_1/n_2)t_\mathrm{r}$, where n_1 and n_2 are co-prime integers, the wave packet may be approximately rewritten as an equally weighted sum of subsidiary wave packets. These are the so called fractional revivals.

4.2. Quantum collapse and revival sequences

To apply the preceding ideas to the particular case of Gazeau–Klauder coherent states for the position dependent mass system, we should commence by using the time-evolution operator in Eq. (23) to write the time-dependent wave packets $|s,\xi,t\rangle$ of the coherent states as

$$|s,\xi,t\rangle=\mathrm{e}^{-\mathrm{i}Ht}|s,\xi\rangle=\frac{1}{\sqrt{G(s)}}\sum_{n=0}^{+\infty}\frac{s^{n/2}\,\mathrm{e}^{-\mathrm{i}(\xi+\varepsilon t)e_n}}{\sqrt{\theta_n}}|\phi_n\rangle. \tag{45}$$

In the literature, a convenient way to probe some aspects of the Gazeau–Klauder coherent states during their time evolution is through a study of the autocorrelation function $C(s,a,t)$ defined as the scalar product between the initial coherent states given in Eq. (30) and the previously constructed time-evolved wave packets,

$$C(t) = \langle s,a,t=0|s,a,t\rangle = \frac{1}{G(s)}\sum_{n=0}^{+\infty}\frac{n+1}{n+2}\left(\frac{s}{a}\right)^n \mathrm{e}^{-\mathrm{i}\varepsilon e_n t}. \quad (46)$$

The idea here is attached to the constraint $0 \leq |C(t)|^2 \leq 1$. More precisely, higher values of $|C(t)|^2$, known as the survival function, occur when the wave packets reproduce their initial states. Conversely, low values of $|C(t)|^2$ correspond to the situation of waves that are far from their initial shapes.[58,61] We have substituted Eq. (25) into Eq. (44) and derived the following timescales:

$$\begin{aligned} t_{\mathrm{c}} &= \frac{\pi\hbar}{a}(n_0+1)^3; \\ t_{\mathrm{r}} &= \frac{2}{3}\frac{\pi\hbar}{a}(n_0+1)^4; \\ t_{\mathrm{s}} &= \frac{1}{2}\frac{\pi\hbar}{a}(n_0+1)^5. \end{aligned} \quad (47)$$

One straightforwardly notices from Eq. (47) that all timescales are proportional to the quantum number n_0 of the most probable state, and consequently to the coherent-state parameter s, keeping in mind the observations in Fig. 3. Contrariwise, $t^{(k)}$ are scaled down by the space deformation coefficient a. In the context of highly excited particles, the system may experience the hierarchy $t^{(k)} \ll t^{(k+1)}$.[62] This is the case if one chooses $n_0 = 91$ as the central quantum number. The various timescales are thus found to be $t_{\mathrm{c}} \simeq 0.0039$, $t_{\mathrm{r}} \simeq 0.2420$ and $t_{\mathrm{s}} \simeq 16.6958$ (in microseconds (μs)) for $a = 0.015$. The motion of wave packets of Gazeau–Klauder coherent states propagating in the Coulomb-like potential is simulated using the survival function in Fig. 5. This figure provides us with rich information about the quantum system. One sees that the coherent-state wave packet initially oscillates with a period of $t \approx t_{\mathrm{c}}$. After a few classical oscillations, phase interference leads to the contraction of the wave packet, that is, the collapse phenomenon. The wave packet is revived after a time $t \approx t_{\mathrm{r}}$ and reconstructs its initial form; this is the quantum revival discernible in Fig. 5(b). This revival structure cannot be considered as an ideal one. In our mind, the reason for this is simple. The function given by Eq. (34) that typifies the Gazeau–Klauder coherent states being studied is not a normal Poissonian function compared to

$$P(n,\lambda) = \frac{1}{n!}\lambda^n \mathrm{e}^{-\lambda}. \quad (48)$$

It is obvious that the revival peaks are not as high as expected in Fig. 5. More precisely, as time evolves, they undergo a decay due to higher-order terms in the wave packet expansion that introduce a distortion into the quantum revivals.[62,63] From a closer look at the revival pattern, it emerges that there is a delay during the appearance of the simulated quantum revivals of the system, compared to the theoretical prediction. For example, the fractional and full revivals expected at $t \approx t_{\mathrm{r}}/2 \simeq 0.1210$ and $t \approx t_{\mathrm{r}} \simeq 0.2420$, respectively, actually appear later, at around $t \simeq 0.1410$ and $t \simeq 0.2777$, as displayed in Fig. 5. We have studied the motion of wave packets in the context of low values of the central quantum number.

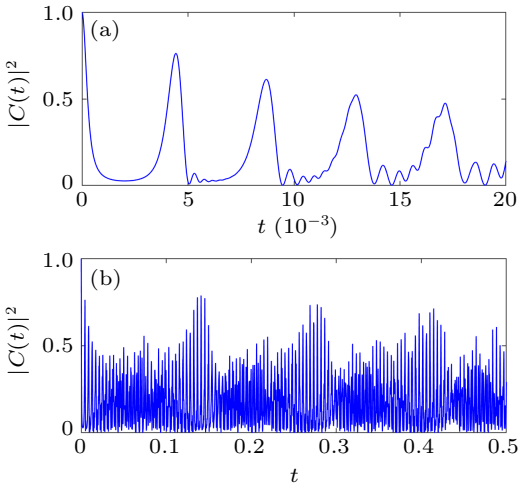


Fig. 5. Plot of the survival function versus time for $s = 0.01$, $a = 0.015$, and $n_0 = 91$, in arbitrary units.

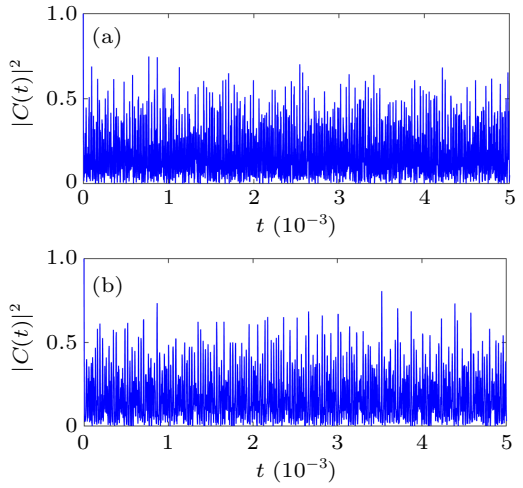


Fig. 6. Plot of the survival function versus time for (a) $n_0 = 5$ and (b) $n_0 = 12$, with $s = 0.01$, $a = 0.015$.

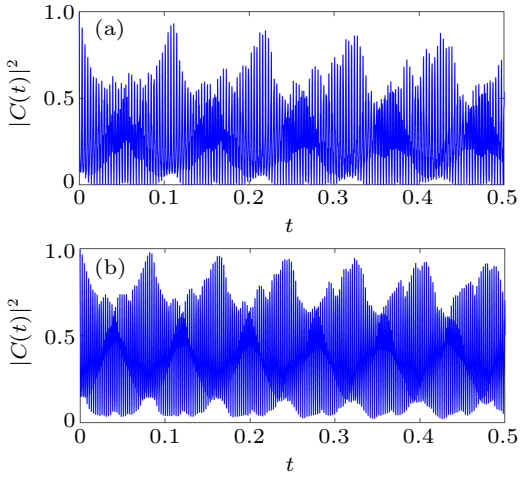


Fig. 7. Plot of the survival function versus time for (a) $a = 0.019$ and (b) $a = 0.025$, with $s = 0.01$, $n_0 = 91$.

It can be seen from Figs. 5 and 6 that regardless of the low or high value of the central quantum number n_0, the revival structure remains evident for a fixed value of the nonlinearity parameter. This observation is in contrast with the results of Naila Amir *et al.* in 2017, when they studied Gazeau–Klauder coherent states of an oscillator in a deformed quadratic potential.[27] On the other hand, an increase of the modified nonlinearity parameter a induces a decrease of the timescales $t^{(k)}$, and consequently an increase of the number of revival cycles for the same duration, as can be seen in Fig. 7. We can now assert that strongly nonlinear systems exhibit more revivals than the others. In what follows, we investigate the behavior of wave packets when the simulation duration is sufficiently increased.

4.3. Long-term evolution of wave packets

We are now interested in the long-term evolution of wave packets for Gazeau–Klauder coherent states in a Coulomb-like potential. The coherent states under consideration are expected to display interesting features at times up to t_s or fractions thereof. In Ref. [62] the reader can find a convincing mathematical explanation that may permit us to predict the revival regime of a quantum-mechanical system. On the other hand, this quantum revival structure can also be predicted by solving the following phase-difference equations:[61]

$$\frac{\mathrm{d}^{b+2}}{\mathrm{d}n^{b+2}}\left[\sum_{k=b+2}^{m}(-1)^{k-1}\frac{(n-n_0)^k}{t^{(k)}}\right]t = \text{integer},\quad t \ll t^{(m+1)}, \tag{49}$$

in which the timescales $t^{(1)}$, $t^{(2)}$, and $t^{(3)}$, respectively, represent t_c, t_r and t_s, while $t^{(4)}$ stands for the timescale corresponding to the fourth-order term in the Taylor expansion of wave packets. Equation (49) gives some approximations for the revival pattern of systems that possess timescales $t^{(k)}$ obeying the hierarchy $t^{(1)} \ll t^{(2)} \ll t^{(3)} \ll t^{(4)}$. For order $b = 0$, this phase-difference equation produces information about quantum revivals with a timescale t_r. The longer timescale, t_s, known as the super-revival time, records the order $b = 1$. Thus Eq. (49) provides us with

$$\frac{6t}{t^{(3)}} = \text{integer},\quad t \ll t^{(4)}, \tag{50}$$

yielding solutions $t = t_s/6, t_s/3$, etc., that exactly match those obtained in Ref. [62]. We have simulated the motion of wave packets for Gazeau–Klauder coherent states in the Coulomb-like potential during the first 8 μs, for which the central quantum number $n_0 = 91$ and the deformation coefficient $a = 0.015$, corresponding to the super-revival timescale $t_s \simeq 16.6958$; the results obtained are displayed in Fig. 8.

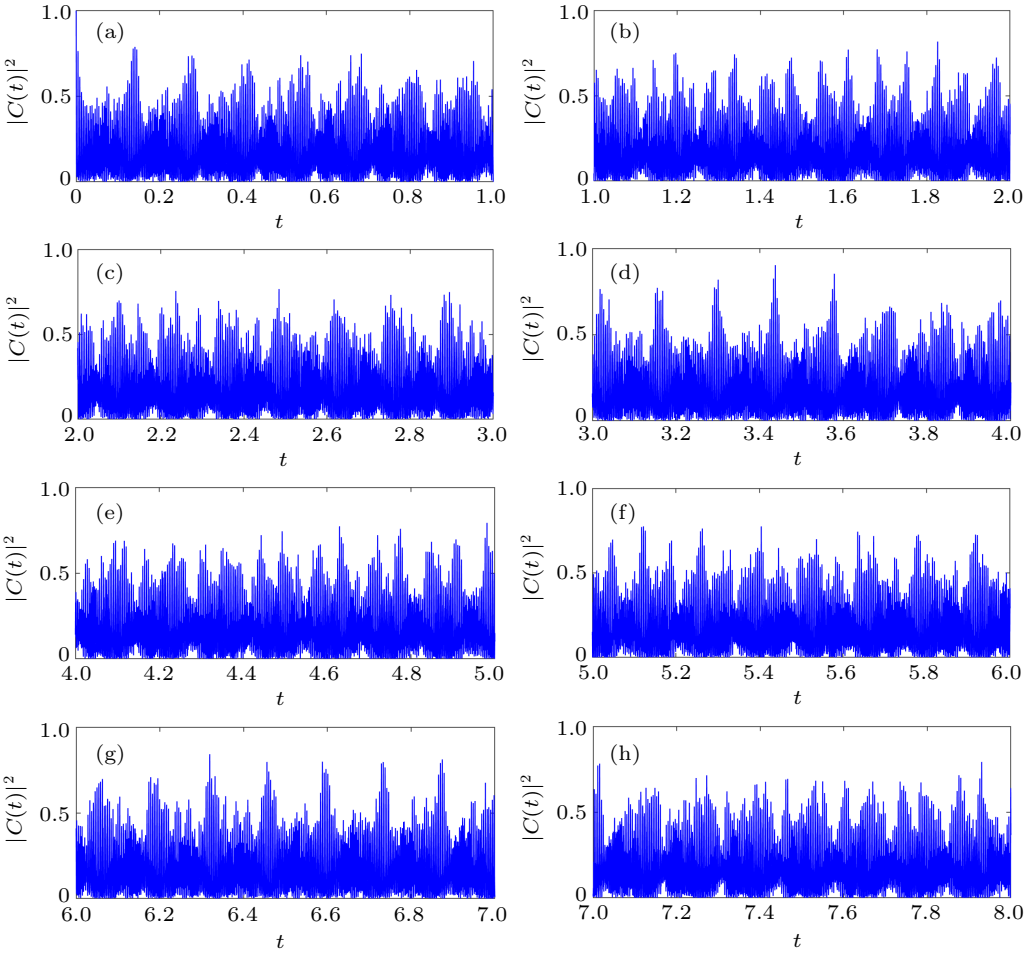


Fig. 8. Plot of the survival function versus time for $a = 0.015$, $s = 0.01$, and $n_0 = 91$ during the first 8 μs.

From this figure, it is easy to see that the full-revival peaks gradually decay in size as well as losing their periodicity. This collapse of wave packets evolves until around $t \simeq 3.4373$ of Fig. 8(d), corresponding to a new sequence of revivals. This sequence later repeats near $t \simeq 6.3190$, as seen in Fig. 8(g), with a peak higher than that of the first revival; this is a super revival. These fractional super revivals were expected to occur at $t \approx t_s/6 \simeq 2.7826$ and $t \approx t_s/3 \simeq 5.5652$, respectively, rather than at $t \simeq 3.4373$ and $t \simeq 6.3190$. This delay can be explained by the loss of periodicity previously mentioned, certainly introduced by the deformation in the coordinate space manifest in the variable changes of Eq. (5). The height of the survival function's peak provides evidence that the super revival looks more like the initial wave packet than the revival packet does, when $t \approx t_r$.

5. Conclusion

This communication focused on Gazeau and Klauder-type coherent states of a mechanical system with a spatially variable mass confined in a potential similar to that of the 1D Coulomb problem. The ensuing energy spectrum appeared in the expected form with an inverse quadratic dependence on n. We found that these energy levels are tightened in strongly nonlinear systems. Using the probability distribution of the photon number revealed that the underlying system exhibits an antibunching phenomenon. Moreover, the temporal evolution of this mechanical system was explored by using the survival function. It was made clear that the wave packets of Gazeau–Klauder coherent states undergo quantum revival and super-revival cycles with a progressive loss in periodicity, consequently leading to their evanescence.

We believe that our work sets the stage for a conceptual and practical understanding of wave packet propagation in systems with position-dependent effective masses in the presence of Coulomb-type confinement potentials. Such systems can be exemplified by bottom-up fabricated atomically-precise segmented graphene nanoribbons, SGNRs. One aspect of this conceptual understanding emanates from both Eqs. (27) and (47), where it is evident that the revival times are proportional to λ^2, a manifestation of time dilation brought about by the non-singular nature of the Coulomb-type potential studied.

Appendix A

Proof of $t^{(k)} < t^{(k+1)}, \quad \forall k$:

Recalling the definition of the timescales:

$$t^{(k)} = 2\pi\hbar \left(\left| \frac{1}{k!} \frac{\mathrm{d}^k e_n}{\mathrm{d}n^k} \right| \right)_{n=n_0}^{-1}, \quad k = 1, 2, 3, \ldots \tag{A1}$$

To verify that

$$\frac{t^{(k)}}{t^{(k+1)}} < 1, \quad \forall k \tag{A2}$$

we define a sequence

$$T_k = \frac{t^{(k)}}{t^{(k+1)}} \tag{A3}$$

for which the first few terms are

$$\frac{3}{2(n_0+1)}; \quad \frac{4}{3(n_0+1)}; \quad \frac{5}{4(n_0+1)}; \quad \cdots \tag{A4}$$

Inspecting the sequence shows that

$$T_k = \frac{2+k}{(1+k)(n_0+1)} < 1, \quad \forall k \tag{A5}$$

hence, Eq. (A2) is true.

References

[1] Xia Y, Yang P, Wu Y, Mayers B, Gates B, Yin Y, Kim F and Yan H 2003 *Adv. Mater.* **15** 353
[2] Amir N and Iqbal S 2020 *J. Math. Phys.* **61** 082102
[3] Tchoffo M, Migueu F B, Vubangsi M and Fai L C 2019 *Heliyon* **5** e02395
[4] Dodin I Y and Fisch N J 2008 *Phys. Rev. E* **77** 1
[5] Andronov A A, Belyantsev A M, Gavrilenko V I, Dodin E P, Krasil'nik E F, Nikonorov V V, Pavlov S A and Shvarts M M 1986 *Zh. Eksp. Teor. Fiz.* **90** 367
[6] Tajmar M and Assis A K T 2015 *J. Adv. Phys.* **4** 77
[7] Zeilinger A, Shull C G, Horne M A and Finkelstein K D 1986 *Phys. Rev. Lett.* **57** 3089
[8] Amir N and Iqbal S 2016 *Commun. Theor. Phys.* **66** 41
[9] Wang J E, Greenwood E and Stojkovic 2009 *Phys. Rev. D* **80** 124027
[10] Meyur S, Maji S, and Debnath S 2014 *Adv. High Energy Phys.* **2014** 1
[11] Peña J J, Morales J, Garcia-Ravelo J and Arcos-Diaz L 2012 *Int. J. Phys. Math. Sc.* **11** 338
[12] Vubangsi M, Tchoffo M and Fai L C 2014 *Eur. Phys. J. Plus* **130** 07
[13] Dong S H 2007 *Factorization method in quantum mechanics* p. 307
[14] Cooper F, Khare A and Sukhatme U 1995 *Physics Reports* **251** 267
[15] Tchoffo M, Vubangsi M and Fai L C 2014 *Phys. Sci. Int. J.* **4** 1370
[16] Tchoffo M, Vubangsi M and Fai L C 2014 *Eur. Phys. J. Plus* **129** 105
[17] Amir N and Iqbal S 2015 *Commun. Theor. Phys.* **111** 20005
[18] Balantekin A B 1998 *Phys. Rev. A* **57** 4188
[19] Aleixo A N F and Balantekin A B 2007 *J. Phys. A: Math. Theor.* **40** 3463
[20] Palma G and Raff U 2006 *Can. J. Phys.* **84** 787
[21] Loinaz W and Newman T J 1999 *J. Phys. A: Math. Gen.* **32** 8889
[22] Jaramillo B, Martinez-y-Romero R P, Nunez-Yepez H N and Salas-Brito A L 2009 *Phys. Lett. A* **374** 150
[23] Imbo T D and Sukhatme U P 1985 *Phys. Rev. Lett.* **54** 2184
[24] Morales J, Peña J J and Lopez-Bonilla J L 2003 *J. Mol. Struct. (TeoChem)* **621** 19
[25] Dai Xianxi, Jixin Dai and Jiqiong Dai 1997 *Phys. Rev. A* **55** 2617
[26] Reyes J A and del Castillo-Mussot M 1999 *J. Phys. A: Math. Gen.* **32** 2017
[27] Amir N and Iqbal S Commun 2017 *Commun. Theor. Phys.* **68** 181
[28] Monir H B, Amir N and Iqbal S 2019 *Int. J. Theor. Phys.* **58** 1776
[29] Ali S T, Antoine J P and Gazeau J P 1999 *Coherent States, wavelets and their applications* p. 385
[30] Combescure M and Robert D 2012 *Coherent States and Applications in Mathematical Physics* p. 431
[31] Perelomov A 2012 *Generalized coherent states and their applications* p. 332
[32] Gazeau J P 2009 *Coherent states in quantum physics* p. 360
[33] Roos O V 1983 *Phys. Rev. B* **27** 7547
[34] Costa Filho R N, Almeida M P, Farias G A and Andrade Jr J S 2011 *Phys. Rev. A* **84** 050102(R)
[35] Mustafa O and Mazharimousavi S H 2007 *Int. J. Theor. Phys.* **46** 1786
[36] Ball C J, Loos P and Gill P M W 2017 *Phys. Chem. Chem. Phys.* **19** 3987
[37] Glick A J, Cohen R J and Bryant G W 1988 *Phys. Rev. B* **37** 2653

[38] Derezinski J 2013 *Ann. Henri Poincaré*
[39] Dereziński J and Richard S 2018 *Ann. Henri Poincaré* **19** 2869
[40] Knospe O and Schmidt R 1996 *Phys. Rev. A* **54** 1154
[41] Rajabi A A and Hamzavi M 2013 *J. Theor. Appl. Phys.* **7** 17
[42] Downing C A and Portnoil M E Phys 2014 *Phys. Rev. A* **90** 052116
[43] Lombard R J, Mezhoud R and Yekken R 2009 *Phys. Scr.* **80** 065005
[44] Haines L K and Roberts D H 1969 *Am. J. Phys.* **37** 1145
[45] Gradshteyn I S and Ryzhik I M 2007 *Table of Integrals, Series, and Products* p. 1221
[46] Nieto M M 2000 *Phys. Rev. A* **61** 034901
[47] Nouri S 2002 *Phys. Rev. A* **65** 062108
[48] Klauder J and Skagerstam B 1985 *Coherent states: Applications in physics and mathematical physics* p. 927
[49] Zhang X Z, Wang Z H, Li H, Wu Q, Tang B Q, Gao F and Xu J J 2008 *Chin. Phys. Lett.* **25** 3976
[50] Mandel L 1979 *Opt. Letters* **4** 205
[51] Ghosh S 2012 *J. Math. Phys.* **53** 062104
[52] Penninia F and Plastino A 2014 *Revista Mexicana de Física E* **60** 103
[53] Bihu L V, Huichao Z, Lipeng W, Chunfeng Z, Xiaoyong W, Jiayu Z and Min X 2018 *Nat. Comun.* **9** 1536
[54] Knospe O and Schmidt R 1996 *Phys. Rev. A* **54** 1154
[55] Venugopalan A and Agarwal G S Phys 1999 *Phys. Rev. A* **59** 1413
[56] Maninder K, Bindiya A and Arvind 2018 *Eur. Phys. J. D* **72** 136
[57] Bluhm R, Kosteleckỳ A and Porter J A 1996 *Am. J. Phys.* **64** 944
[58] Robinett R W 2004 *Physics Reports* **392** 1
[59] Roy U, Banerji J and Panigrahi P K 2005 *J. PhysA: Math. Gen.* **38** 9115
[60] Averbukh I Sh and Perelman N F 1989 *Phys. Lett. A* **139** 449
[61] Aronstein D L and Stroud-Jr C R 2005 *Las. Phys.* **15** 1496
[62] Bluhm R and Kosteleckỳ V A 1995 *Phys. Rev. A.* **51** 4767
[63] Vrakking M J. J., Villeneuve D M and Stolow A 1996 *Phys. Rev. A* **54** R37